FUNDAMENTALS of SOLAR CELLS

Photovoltaic Solar Energy Conversion

(2)

ALAN L. FAHRENBRUCH
RICHARD H. BUBE

CHAPTER 7

SILICON SOLAR CELLS

Among all the semiconductors, the properties of silicon are the most widely known, and conceptually, the silicon homojunction solar cell is perhaps the simplest of all photovoltaic devices. In 1981 the Si p/n junction cell was the only solar cell widely available commercially. The cost of Si cells was \$10–\$15 per peak watt in 1983 for terrestrial arrays, in spite of relatively inexpensive raw materials and a fairly well-developed technology.

This chapter begins with a short historic perspective on the development of the Si cell. The purification and crystal growth of Si are treated in some detail to illustrate the complexities and the wealth of options involved in obtaining a semiconductor material of high purity and low defect density. The electrical properties of several representative device types and a sample processing sequence are included to demonstrate the interaction between electrical parameters and processing. The chapter concludes with a section outlining the optimization of cell properties both by fine-tuning the parameters of "standard" cell designs and by innovative approaches of a more basic nature.

7.1 HISTORY

There was already an appreciation for future need when the Si solar converter was invented at Bell laboratories in 1953. At that time D. M. Chapin was investigating power sources for remote communication systems while C. S. Fuller was exploring solid-state diffusion as a means

of producing large-area p/n junctions in Si. Then G. L. Pearson, in his investigations of power rectifiers made by Fuller's techniques, noticed the extreme sensitivity to light of these devices and matched solution to need. When Pearson's diode (a Li-diffused n-on-p structure) was tested in sunlight, a solar conversion efficiency of $\simeq 4\%$ was obtained—some five times more efficient than previously known Se cell converters. Because of the high atomic diffusivity of Li the devices were somewhat unstable, however, even at room temperature. Fuller developed a boron diffusion technology, and, in 1954, Chapin *et al.* (1954) published a description of a 6% efficient, stable Si solar cell. The first practical trial was a 9-W array powering a telephone repeater installed in Americus, Georgia, in 1955. During 6 months of use it was a technical success, but it proved to be an uneconomical power source for the intended use.

The Sputnik era provided the impetus to continue Si cell research; the first use of solar photovoltaic converters in space occurred on March 17, 1958, when Vanguard I was put into orbit. Its solar-powered radio transmitter operated for 8 years before radiation damage to the cells stopped its signals.

Since that time the cost of Si cells has rapidly decreased as the technology has developed (Fig. 7.1) and the efficiencies have risen to the 15–17% level for space cells (AM0). Until 1977, when GaAs cells were first used on a few Russian satellites, the only serious competitor for Si cells had been the Cu_xS/CdS all-thin-film cell, which promised increased radiation resistance but failed to reach high enough efficiency levels to penetrate the space market. With the advent of terrestrial photovoltaics the picture has again become more complex, and many devices, including GaAs concentrator systems and various thin-film cells, are being investigated as possible economical alternatives to the single-crystal Si cell.

One trend for commercial Si cells in the past few years has been to "fine-tune" orthodox devices, principally by decreasing short-wavelength losses in the front n-type layer, increasing the obtainable V_{oc} by manipulation of doping levels, and increasing resistance to radiation damage.

The detailed history of technological improvement of the Si cell is beyond the scope of this book; the interested reader is referred to articles by Wolf (1972) and Smits (1976). However, a few of the notable improvement milestones have been the "standard" n/p cell ($\eta_s = 10.4\%$ at AM0), the "violet cell" (14%), and the Comsat nonreflecting (CNR) cell (16%). A fourth major milestone was the use of a "back-surface electric field" (BSF) to decrease carrier loss at the back surface of the cell, an idea conceived in 1960 (Dale and Rudenberg, 1960) but practically demonstrated by Mandelkorn and Lamneck (1972).

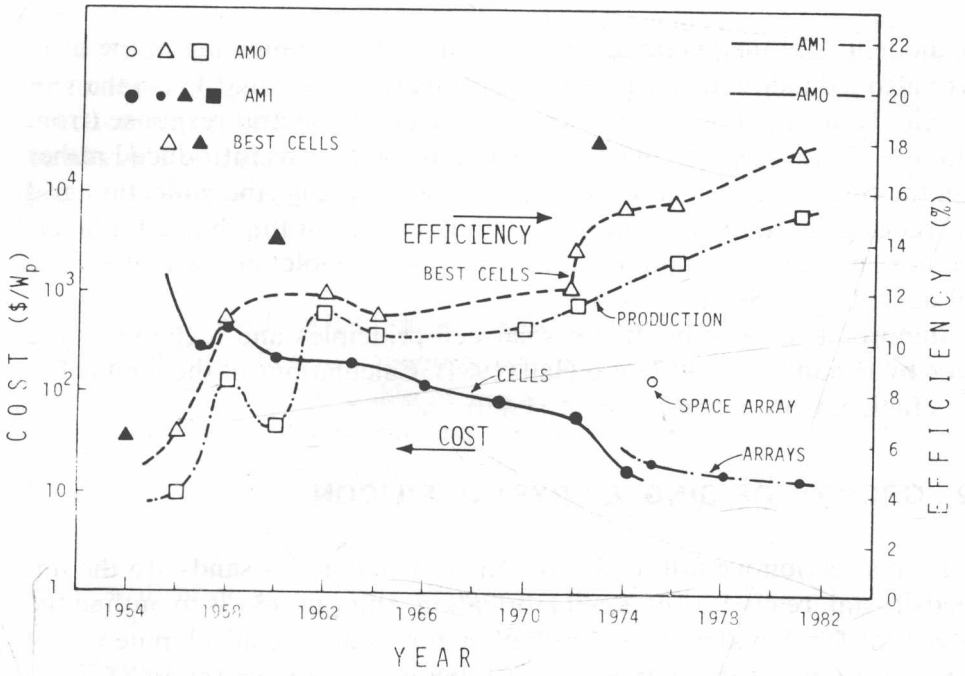

Fig. 7.1. Single-crystal silicon cell solar efficiency and cost per peak watt for cells and arrays over the years. $T \simeq 300°K$. Costs are given for the year in which they are quoted; inflation is not accounted for. Cost data are for terrestrial cells and arrays except for a 1975 datum for a space array. [Much of the early data is redrawn from Wolf (1972). The remainder is drawn from a variety of sources. The AM0 and AM1 efficiency lines at the top of the figure are practical maximum design goals by M. Wolf, *IEEE Trans. Electron Devices* **ED-27**, 781 (1981).]

The violet cell, developed at Comsat by Lindmayer and Allison (1973), serves to illustrate the direction of these improvements. The response to blue-violet light in this cell is substantially enhanced relative to its predecessors by decreasing the thickness of the diffused n-type front layer to 0.1–0.2 μm and by increasing the minority carrier lifetime there. In previous cells the diffusion of P to depths of $\simeq 0.5$ μm was accompanied by the formation of a "dead layer" $\simeq 0.1$ μm thick, where the P concentration approached the solubility limit in Si and the hole lifetime was about 10^{-10} sec. Dislocations propagating from the dead layer were thought to penetrate the depletion region, forming additional recombination centers there.† Although these latter centers did not appreciably affect J_L, they did increase the space-charge-region recombination current, increasing

† This view has been questioned and the "dead layer" is now thought instead to be due to phosphorus-vacancy pairs, various precipitates, and Auger recombination.

the diode loss at the maximum power point. Thus elimination of the dead layer also led indirectly to a considerable increase in ff and V_{oc} in the violet cell. To accommodate the increased range of spectral response (from 0.45 to 0.35 μm) an antireflection coating of Ta_2O_5 was introduced rather than the SiO_x or TiO_x coatings formerly used. Finally, the collection grid was redesigned to offset the reduced conductivity of the thinned n-layer. The next principal escalation in efficiency of the violet cell was the CNR cell described in Section 7.4.4.

Important reviews of silicon solar cell principles and technology are given by Brandhorst (1977) and Hall (1981). Calculations of the limits of Si cell efficiency are given by Wolf (1980).

7.2 GROWTH OF SINGLE-CRYSTAL SILICON

In this section we follow Si from the raw material—sand—to the finished crystal, ready for solar cell fabrication. Our purpose is to outline the procedure for a material in a rather mature stage of development and therefore to gain some perspective on the possible preparation of other less-well-researched materials.

7.2.1 Sand to Silicon

The word *silicon* comes from the Latin *silex*, meaning "flint." Silicon is the second-most abundant element, comprising about 20% of the earth's crust, mainly in the form of SiO_2-based minerals (quartzite, agate, jasper, opal, and flint) and silicates (micas, feldspars, zeolites, garnets, and clays). Silicates are the major constituents of glass. Although Lavoisier suggested that SiO_2 was the oxide of a then unknown element (ca. 1787), it was 1823 before Si was first isolated by Berzelius.

The present-day uses of elemental Si are principally in steelmaking, in the production of SiC abrasives, and in silicones. The use of elemental Si for optical components for infrared transmission served as an impetus for single-crystal growth technology until methods were discovered to make polycrystalline optical material with low infrared loss. Its first use as an electronic component appears to be as a point contact rectifier in 1906. Despite the rapid expansion of the semiconductor industry, relatively little tonnage is used there: 45 tons in 1964, 500 tons in 1972, and $\approx$1500 tons in 1978.

Silicon is a light, brittle element that is ductile only when heated relatively close to its melting point of 1410°C. The element is very resistant to chemical attack. A layer of SiO_2 10–20 Å thick forms almost immediately on exposure to air, then more and more gradually increases in thickness

to 50–60 Å. Silicon is not attacked by common acids except a mixture of HF and HNO_3, but it is quite soluble in KOH or NaOH, liberating H_2. The material takes a high optical polish rather easily, but the high index of refraction makes antireflection coatings necessary on optical elements. The physical and electronic properties of Si are listed in Table 7.I and the optical absorption constant is shown in Fig. 3.8.

The transformation of raw sand to high-purity Si involves the following general steps:

(1) reduction of SiO_2 to impure Si with C in an electric arc furnace,
(2) transformation to a chemical intermediate such as trichlorosilane,
(3) purification by distillation and other means,
(4) reduction of the intermediate to Si under high-purity conditions,
(5) casting into a form suitable for crystal growth, and
(6) crystal growth, providing an additional purification step by segregation of certain of the impurities.

These purification steps bring impurity levels from between 1 and 10% down to the parts per billion range. Standard analytical techniques such as emission spectroscopy are much too crude to measure impurity concentration at this level and sophisticated techniques such as mass spectroscopy and neutron activation analysis must be used. Often the electrical properties of the finished bulk crystal or the device are used to monitor the ultimate impurity levels. Particular attention is paid to elements from columns III-A and V-A, which act as dopants, and to strong recombination centers ("lifetime killers") such as Au, Cu, and Fe.

The reduction of SiO_2 to Si with C in an electric arc furnace is a large-volume industrial process (200,000 tons per year in the United States in 1973) yielding up to 98–99% pure Si at prices of $\simeq$\$1 kg^{-1}. There have been promising attempts at preliminary purification for solar cell destined material by unidirectional solidification of the arc furnace pour-off (Hunt *et al.*, 1976). Many methods exist by which the metallurgical-grade Si is reacted to form compounds that can be more easily purified. Most include Si/halogen compounds since these are gaseous or liquid at low temperatures and a large degree of purification can be effected by simple distillation. The purified compound is then reduced with H_2, an active metal, or pyrolytically. Representative of such reactions are

$$SiCl_4 + Zn, Al, \text{ or } H_2 \rightarrow Si + ZnCl_2, Al_2Cl_3, \text{ or } HCl$$
$$SiHCl_3 + H \rightarrow Si + HCl$$
$$SiH_4 \text{ (pyrolysis)} \rightarrow Si + H_2$$
$$SiI_4 \text{ or } SiBr_4 + H_2 \text{ (or pyrolysis)} \rightarrow Si + HI \text{ or } HBr \text{ (or } I_2 \text{ or } Br_2)$$
$$SiCl_4 + LiAlH_4 \rightarrow SiH_4 + LiCl + AlCl_3$$
$$\hookrightarrow \text{pyrolysis} \rightarrow Si + H_2$$

Table 7.I

Physical and Electronic Properties of Si[a]

Physical and optical properties			
Crystal form	Diamond cubic		
Lattice constant	5.431 Å		
Melting point	1412°C		
Boiling point	3145°C		
Thermal expansion coefficient	2.33×10^{-6} °C^{-1}		
Thermal conductivity	1.41 W cm^{-1} °C^{-1}		
Density	2.328 g cm^{-3}		
Index of refraction	$\simeq 3.5$ ($\lambda > hc/E_g$)		
Expansion on freezing	9% volume		
Electric parameters		Practical[b]	Typical maximum observed values
E_g, direct	2.6 eV	-	
E_g, indirect	1.12 eV		
dE_g/dT	-2.8×10^{-4} eV °C^{-1}		
μ_e	—	500–700	1360 cm^2 V^{-1} sec^{-1}
μ_h	—	200–350	495 cm^2 V^{-1} sec^{-1}
ϵ_r (dc)	11.7	—	
τ_{n0}[d]	—	5–80	800 μsec
τ_{p0}[d]	—	5[c]	15 μsec
χ	4.01 eV		
n_i[e]	1.4×10^{10} cm^{-3}		
N_c	2.86×10^{19} cm^{-3}		
N_v	1.02×10^{19} cm^{-3}		
Effective masses			
Electrons			
Longitudinal	0.98		
Transverse	0.19		
Conductivity	0.26		
Density of states	0.33		
Holes			
m^*_{heavy}	0.49		
m^*_{light}	0.16		
$m^*_{spin-orbit}$	0.24		
Density of states	0.55		

[a] All properties at 300°K unless inapplicable.

[b] In fabricated solar cells.

[c] In a diffused layer, hole lifetime is reduced to 0.001 to 0.1 μsec.

[d] See Section 3.5.2.

[e] The intrinsic carrier density is given by $n_i = 3.87 \times 10^{16}\, T^{3/2} \exp(-0.605/kT)$. [R. A. Smith, *Semiconductors*, Cambridge Univ. Press. (1959), p. 359.]

Several of these reactions have serious drawbacks in that the reactants are expensive (SiI_4 or $SiBr_4$), yields are low, or the products are dangerous. Runyan (1965) and Wolf *et al.* (1976) provide more information about these and other Si processes.

A widely used commercial method is based on the simplified reaction

$$\left.\begin{matrix} SiCl_4 \\ \text{or } 2SiHCl_3 \end{matrix}\right\} + 2H_2 \xrightarrow[\text{Heat}]{} \left\{\begin{matrix} Si + 4HCl \\ \text{or } 2Si + 6HCl. \end{matrix}\right.$$

The Si is chlorinated in a fluidized bed forming $SiCl_4$, which is then distilled at $\simeq 58°C$ (with some possible intervening purification steps) and finally deposited on hot quartz, Ta, or, more often, an rf induction-heated Si rod in the presence of H_2 at $\simeq 950°C$. The latter procedure has the advantage of eliminating the casting step discussed later.

In some cases the purified Si must be formed into a shape favorable to crystal growth by casting. This step can introduce considerable difficulty. Hot molds are not good since molten Si dissolves all metals to some degree and there is even slow dissolution of SiO_2 crucibles, which adds impurities present in the SiO_2 to the melt. Si has a 9% increase in volume on freezing so that SiO_2 molds are destroyed on cooling. Si_3N_4 and SiC have been used with some success for hot molds. Some casting is done using cold molds so that impurities are confined to the surface layers (Runyan, 1965).

Figure 7.2 shows the cost of Si versus impurity content. Research has been carried out to specify a "solar grade" of Si in which the primary consideration is lifetime rather than the general high-purity, low-defect concentration requirements of integrated circuit fabrication (Wakefield *et al.*, 1975). It is the purpose of these research efforts to identify which impurities and what impurity concentrations are deleterious to solar cell efficiency (Hill *et al.*, 1976).

The growth of single crystals of Si can be accomplished by a wide variety of methods involving growth from gas, liquid, or solution (see, e.g., Runyan, 1965, p. 29). The two most widely used techniques for Si, Czochralski (CZ) and float zone (FZ), are discussed briefly here. Several of the more unusual techniques, aimed at formation of thin layers without slicing, are mentioned as well.

In the process of crystal growth it is desirable for solidification to occur as close to thermal equilibrium as possible. Crystal growth can be divided into three broad categories:

1. *Single-Component Systems.* Material is solidified from its own liquid or vapor.

2. *Multicomponent Systems.* Material is frozen out of a supersaturated solution, e.g., Si from In.

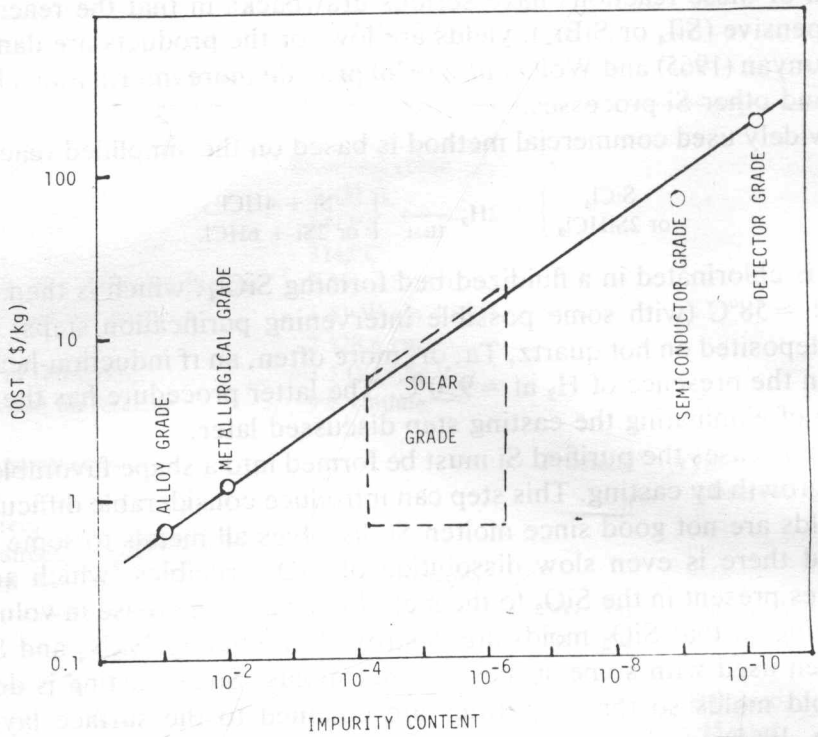

Fig. 7.2. Cost of Si versus purity, used in the identification of a "solar-grade" material (before crystal growth). [Redrawn from G. F. Wakefield, P. D. Maycock, and T. L. Chu, *Proc. 11th IEEE Photovoltaic Specialists Conf.* (1975), p. 49. © 1975 IEEE.]

3. *Multicomponent Reactive Systems.* Material is formed by a reaction in a vapor or liquid phase close to or at the growth site, e.g., $SiH_4 \rightarrow Si + 2H_2$ by pyrolysis.

The basic example of the first category is the Bridgman technique in which solidification occurs as a closed tube containing the molten liquid is passed slowly through a temperature gradient. This technique cannot be used for Si, however, because of dissolution of the tube, sticking to the walls, and expansion on freezing.

To avoid these problems much of the Si is grown today by the Teale–Little modification of the Czochralski method in which the effect of the container is partially eliminated by pulling the freezing crystal from the melt, Fig. 7.3. The container is eliminated altogether in the float-zone process, where surface tension is used to contain a thin moving zone of molten Si in a cylinder of the material.

In crystal growth from the liquid material there are two primary factors controlling growth rate. The first, latent heat removal, is the major

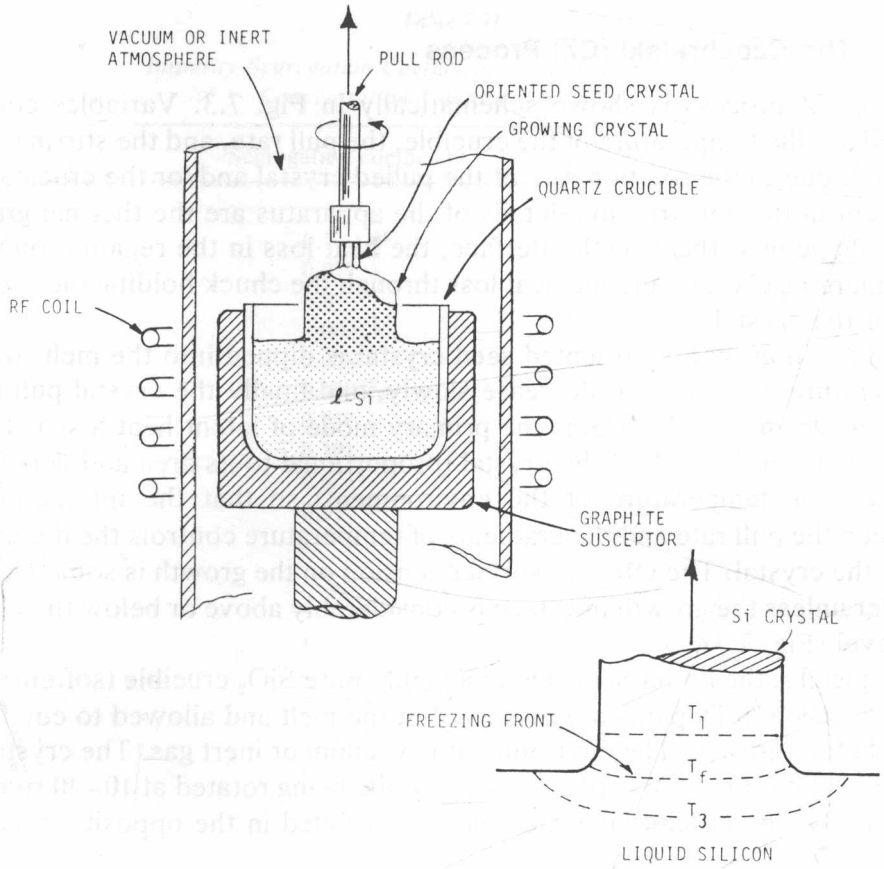

Fig. 7.3. Schematic of Czochralski crystal-growing apparatus.

rate-limiting step. The second, the time necessary for atoms in the liquid to diffuse to an appropriate crystal site, is usually minor in systems in which the liquid is not supercooled. The diffusion time is different for different crystal faces; this generally produces artifacts on the boule and may influence the impurity distribution. Many other factors, including the shape and magnitude of the temperature gradient in the liquid and the solid, the impurity concentration, crystalline line and surface defects, and the shape of the growth interface, influence the growth more or less strongly.

As a greater portion of the liquid is supercooled, the influence of these factors can become dominant. For example, dendritic growth is controlled by sets of twin planes that facilitate the selection of available nucleation sites in a supercooled melt where the growth rate is extremely fast. Similarly, whisker growth from the vapor is seen in which a single screw dislocation provides an axis for rapid nucleation.

7.2.2 The Czochralski (CZ) Process

The CZ process is shown schematically in Fig. 7.3. Variables controlled are the temperature of the crucible, the pull rate, and the stirring of the melt due to the rotation rate of the pulled crystal and/or the crucible. Inherent in the construction details of the apparatus are the thermal gradient shape near the growth interface, the heat loss in the region around the emerging crystal, and the heat loss through the chuck holding the seed end of the crystal.

To begin growth an oriented seed crystal is dipped into the melt, the temperature is allowed to decrease slowly, and finally the crystal pull is initiated. In most CZ systems the primary mode of latent heat loss is by radiation from the bulk of the crystal (proportional to its area and dependent on the temperature of the environment) so that the interaction between the pull rate and the gradients of temperature controls the diameter of the crystal. The effect of surface tension on the growth is somewhat smaller unless the growth interface is considerably above or below the liquid level (Fig. 7.3).

Typically, the liquid Si is held in a highly pure SiO_2 crucible (softening point $\simeq 1600°C$). Dopants are dissolved in the melt and allowed to equilibrate before growth. The environment is vacuum or inert gas. The crystal is pulled at a rate of $10^{-4}-10^{-2}$ cm sec^{-1} while being rotated at 10–40 rpm. Frequently, the crucible is simultaneously rotated in the opposite direction.

Perhaps the best crucible material at present is quartz. Quartz dissolves slowly in the liquid Si with the reaction

$$2SiO_2 \rightarrow 2SiO + O_2$$

until the melt is saturated with oxygen ($2-4 \times 10^{18}$ cm^{-3}) (Runyon, 1965, p. 18) and then only SiO is formed. The SiO vaporizes while impurities from the dissolved quartz are incorporated into the melt. The use of as small a surface-to-volume ratio as possible and of very pure quartz is desirable. Carbon has been used as a crucible material, but is somewhat soluble in Si, producing SiC inclusions. Impurities may also be introduced because of the difficulty in purifying the carbon.

Boules up to 12 inches in diameter and several meters long have been grown by the CZ process.

7.2.3 Impurity Segregation

Impurities from the melt are segregated linearly across the freezing interface so that

$$N_S = k_0 N_L \tag{7.1}$$

Table 7.II

Impurity Segregation Coefficients, Solubility Limits, and Concentration Tolerances in Silicon

Impurity	Segregation coefficient	Solubility limits	Tolerance[e]
Dopants			
O	0.5–1.0[b]	2×10^{18}[b]	
C	0.07[d]	9×10^{17}[d]	
B	0.8[a]	—	
Al	0.002[a]	2×10^{19}[d]	
Ga	0.008[a]	—	
In	0.0004[a]	—	
P	0.35[a]	—	
As	0.30[a]	—	
Sb	0.023[a]	10^{19}[b]	
Li	0.01[b]	—	
Lifetime killers			
Au	—	—	7×10^{14}
Cr	10^{-5}	5×10^{15}	5×10^{15}
Cu	4×10^{-4}	10^{17}	1×10^{15}
Fe	8×10^{-6}	3×10^{16}	1×10^{15}
Mg	2×10^{-3}	5×10^{18}	$>2 \times 10^{15}$
Mn	10^{-5}	4×10^{16}	2×10^{16}
Na	2×10^{-3}	9×10^{18}	2×10^{14}
Ni	10^{-4}	10^{17}	$>4 \times 10^{16}$
Ti	10^{-5}	10^{15}	4×10^{13}
V	10^{-5}	5×10^{15}	1×10^{14}
Zr	—	—	4×10^{13}
C	—	—	$\approx 1 \times 10^{17}$

[a] H. J. Hovel, "Solar Cells," Semiconductors and Semimetals, Vol. 11. Academic Press, New York, 1975.

[b] W. R. Runyan, "Silicon Semiconductor Technology," pp. 18, 108. McGraw-Hill, New York, 1965.

[c] G. F. Wakefield, P. D. Maycock, and T. L. Chu, *Proc. 11th IEEE Photovoltaic Specialists Conf.* (1975), p. 49.

[d] D. E. Hill, H. W. Gutsche, M. S. Wang, K. P. Gupta, W. F. Tucker, J. D. Dowdy, and R. J. Crepin, *Proc. 12th IEEE Photovoltaic Specialists Conf.* (1976), p. 112. More complete data on solubility vs. temperature in Si will be found in F. A. Trumbore, *Bell Syst. Tech. J.* **39,** 205 (1960).

[e] Based on permissible impurity concentration such that a $\eta_s \approx 10\%$ efficient solar cell can be fabricated from B-doped 0.5-Ω cm material. From D. E. Hill *et al., Proc. 12th IEEE Photovoltaic Specialists Conf.* (1976), p. 112.

at the interface, where N_S and N_L are the impurity concentrations in the solid and the liquid and k_0 is the equilibrium segregation coefficient, examples of which are shown in Table 7.II. In the CZ case the remaining impurities are concentrated in the melt, and, for the simple situation of

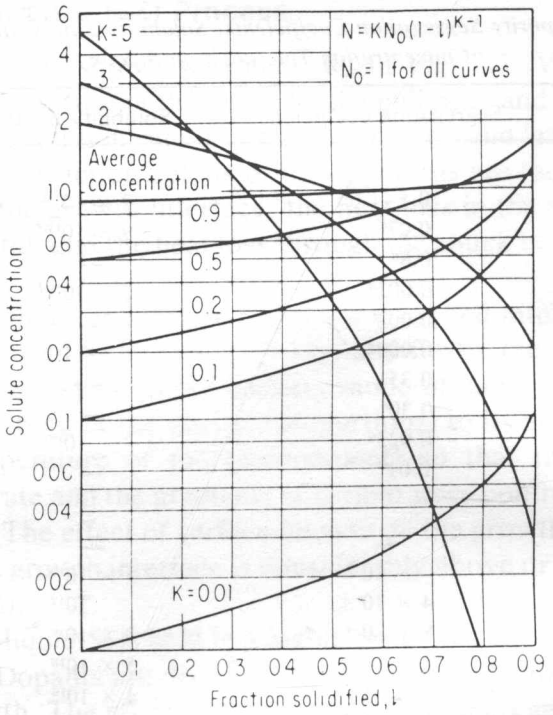

Fig. 7.4. Impurity concentration versus the fraction of the melt-solidified z (e.g., the CZ process). [After W. G. Pfann, "Zone Melting," 2nd ed. Wiley, New York, 1966.]

one-dimensional freezing,

$$N_S(z) = N_0 k_0 (1 - z)^{(k_0 - 1)}, \tag{7.2}$$

where N_0 is the impurity concentration in the melt before growth and z is the fraction of the melt frozen. This relation is plotted in Fig. 7.4. Note that a low k_0 is required to remove impurities from the melt, whereas a high k_0 is required for uniform doping. Too high a concentration of a doping impurity may inhibit single-crystal growth, however; for example, $\gtrsim 2\%$ Sb will prevent Si from growing as a single crystal. For this reason B is preferred over Al as a dopant for CZ growth.

In the float-zone (FZ) process to be discussed next, impurities accumulate in the molten zone since they are being added at a rate $N_0\,dx$ at the melting front of the zone while at the freezing end they are being incorporated at a rate $k_0 N_L\,dx$. The relation for the case of impurity removal is

$$N_S(x) = N_0\{1 - (1 - k_0)\exp[-k_0 x/x']\}, \tag{7.3}$$

where x' is the length of the molten zone and x is the distance along the rod. This relation is plotted in Fig. 7.5. A single FZ pass is not as effective

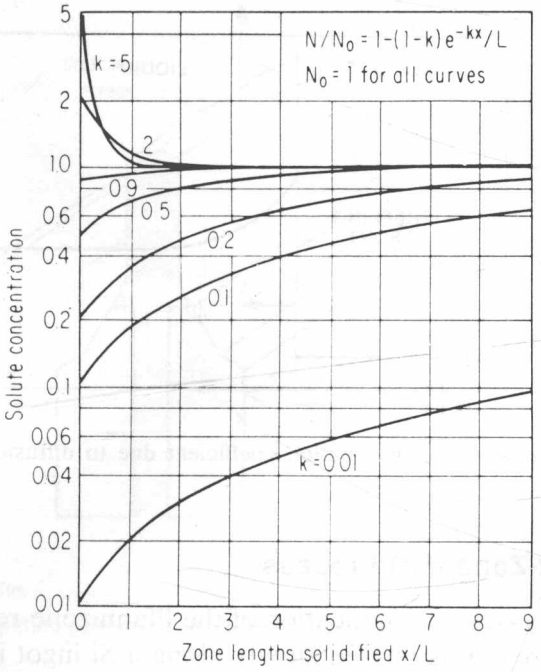

Fig. 7.5. Impurity concentration versus distance along a zone-refined rod (normalized by zone length L'). [After W. G. Pfann, "Zone Melting," 2nd ed. Wiley, New York, 1966.]

as CZ in removing impurities but in the FZ case it is much easier to make repeated passes to purify the crystal.

When it is desired to dope the FZ crystal intentionally the relation is

$$N_S = k_0 N_d \exp(-k_0 x/x'), \tag{7.4}$$

where N_d is the initial doping concentration in the zone. For N_S to be nearly constant with distance, the concentration in the zone must be almost constant and a low segregation coefficient is required in contrast to the CZ case. One method of circumventing this difficulty is to distribute dopant along the rod in a series of sawed notches before zoning so that the dopant is replenished as growth proceeds. Other methods are by addition of a dopant gas (e.g., PH_3 or B_2H_6) to the growth ambient or by neutron transmutation doping (NTD).

During growth the impurity is constantly being rejected at the freezing front. It must be transported back into the bulk of the liquid by diffusion so that a concentration gradient develops near the growth interface. This effectively increases k by a factor depending on the growth rate and stirring speed (see Fig. 7.6). The ratio of k_{eff}/k_0 can range from 1 to 4 for commonly used growth and stirring rates (Runyan, 1965).

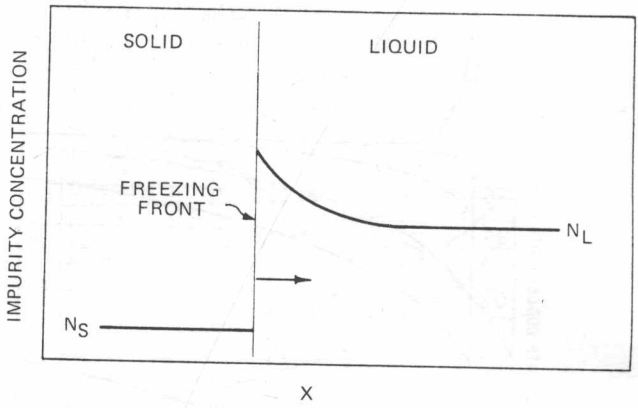

Fig. 7.6. Enhanced effective distribution coefficient due to diffusion near advancing freezing front.

7.2.4 The Float-Zone (FZ) Process

In the FZ processes, a modification of the Pfann zone-refining method, a narrow molten region is passed slowly along a Si ingot in a vacuum or inert gas environment. The ingot is held in a vertical position and the heat is supplied by rf induction. The molten Si is held in place both by surface tension and by the levitation effect of the rf field. Similar considerations with respect to control of lateral and radial temperature gradients and growth rate hold as for CZ. FZ crystals have a somewhat higher purity than CZ material due to the absence of contamination from a crucible; in particular the oxygen concentration can be reduced by a factor of 20–100. Minority carrier lifetime and mobility also tend to be higher than for CZ material. On the other hand, the dislocation density of the FZ material is higher because steeper temperature gradients are involved and because compromises must be made with regard to the temperature profile due to rf heating considerations. These differences are particularly important with respect to radiation resistance effects (Section 7.5.1).

The FZ process starts with a polycrystalline ingot of about the same size as the crystal to be grown. Both the end of the ingot and the end of an oriented seed crystal are locally heated and then skillfully joined, much like the comparable part of the CZ growth. In FZ growth, the heated zone usually travels in the upward direction and is about 2 cm long. The taper from the small seed to the large portion of the crystal is established by the difference in drive rates between the upper chuck, holding the polycrystalline ingot, and the lower chuck, holding the seed. Growth of crystals 50 to 100 cm long and 7.5 cm in diameter is routine, and crystals up to 10 cm in diameter have been grown. The processing is somewhat faster than with CZ growth. A general comparison of CZ and FZ Si growth is given by Matlock (1979).

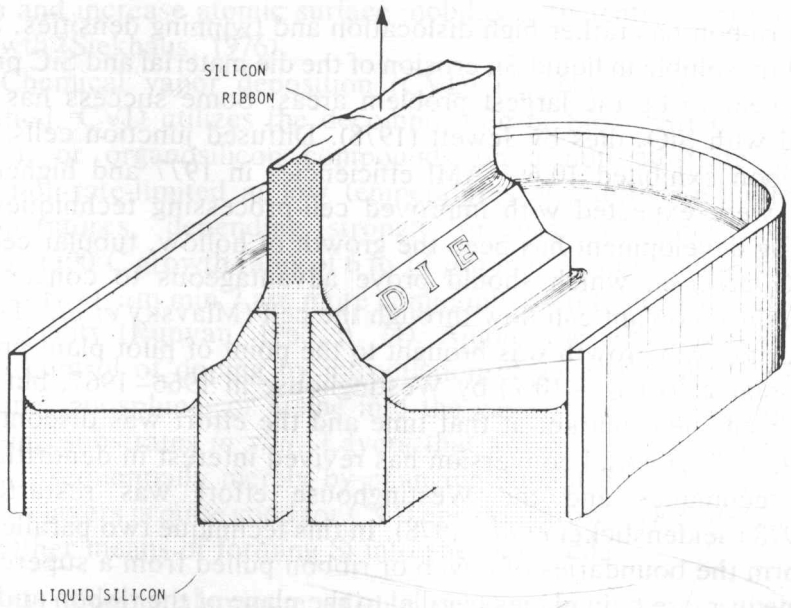

Fig. 7.7. Simplified schematic diagram of edge-fed growth of silicon ribbon.

7.2.5 Other Growth Methods

The expense of slicing and polishing wafers has led to development of methods for the growth of Si directly in the form of thin ribbons by "edge-defined, film-fed growth (EFG)" or by dendritic web growth.

EFG, apparently first applied to Si by Ciszek (1972; Ciszek and Schwuttke, 1975),† has been used as a commercial method for growing sapphire tubes, ribbons, and other cylindrical shapes for a number of years. Si growth by this technique has recently undergone intense development by LaBelle and Mlavsky (1971), and Ravi *et al.* (1975). In this process a carbon die with a slot-shaped aperture is immersed part way in a vessel of molten Si. The liquid Si wets the die and, in operation, flows through the slot to feed the solid zone above as in Fig. 7.7. The shape of the ribbon is controlled by the shape of the top surface of the die, by surface tension, temperature gradients, and the pull rate.

Rates reported in 1980 were up to 5 cm min^{-1} for ribbons 0.05 cm thick and up to 5 cm wide (Kalejs, 1980). Ribbons are flexible enough to be wound on large drums and ribbons 20 m long have been grown in a single run. No polishing is required. Using multiple dies and continuous processing, Mlavsky estimates the potential cost of ribbon at less than \$0.002 cm^{-2}.

† EFG is similar to the Stepanov technique for ribbon growth except that in the latter case the die is not wetted by the Si.

EFG ribbon has rather high dislocation and twinning densities. Since C is slightly soluble in liquid Si, erosion of the die material and SiC precipitates appear to be the largest problem areas. Some success has been achieved with SiO_2 dies by Jewett (1978). Diffused junction cells made from ribbon exhibited 10.6% AMl efficiencies in 1977 and higher efficiencies were expected with improved cell-processing techniques. An interesting development has been the growth of hollow, tubular cells by the EFG process, which should prove advantageous to concentrator systems since coolant can flow through the cell (Mlavsky *et al.*, 1976).

Dendritic web growth was brought to the point of pilot plant production of solar cells ($\eta_s \simeq 10\%$) by Westinghouse in 1966–1967, but there was an insufficient market at that time and the effort was discontinued (Riel, 1973). Terrestrial conversion has revived interest in dendritic web growth techniques and the Westinghouse effort was restarted in 1977–1978 (Seidensticker *et al.*, 1978). In this technique two parallel dendrites form the boundaries of a web or ribbon pulled from a supercooled melt. One or more twin planes parallel to the plane of the ribbon and at its center stabilize the growth (Dermatis *et al.*, 1965) and no dies are needed. Growth rates are $\simeq 10$ cm min^{-1} and widths of 4 cm have been achieved, with area output rates of 27 cm^2 sec^{-1} (Duncan *et al.*, 1980). Temperature control must be very precise. The quality of the ribbon is equal to good CZ material, and the twin planes appear not to be detrimental to the cell efficiency (Seidensticker *et al.*, 1975; Davis *et al.*, 1976). Cells with $\simeq 15.5\%$ efficiency (AM1) have been produced (Duncan *et al.*, 1980).

A technique for exceptionally high-speed growth of Si ribbon has been introduced by Tsuya *et al.* (1980). Using gas pressure, molten Si is squirted from a slot in the bottom of a holding crucible onto a set of cold, rotating rollers, producing ribbons at a rate of 10 to 40 m sec^{-1}! Polycrystalline ribbons 20 to 200 μm thick and 0.1 to 5 cm wide have been grown. The grain size is large (10 to 100 μm) and cells with $\eta_s = 5\%$ (without an antireflection coating) were fabricated from the roller-quenched ribbon in the early stages of research.

Silicon can be grown from solution at somewhat lower temperatures than its melting point using Ga or Sn as a solvent, but rates are low and the technique has not received much attention for solar cells (Wolf, 1975).

When Si films are grown by vacuum evaporation, high source temperature (> 1800°C) and good vacuum ($\lesssim 10^{-7}$ Torr) are required, the latter to prevent formation of SiO. Solar cells grown by this method have reached $\eta_s \simeq 3\%$ (Feldman *et al.*, 1980). A high substrate temperature (> 1000°C) is required as well to achieve epitaxy or large-grain polycrystal growth. Higher temperatures also tend to reduce stacking fault and dislocation densities. The temperature can be reduced by fluxing with thin films of Pt or other metals (several monolayers), which remain on top of the growing